Spontaneous R2* Fluctuations for Non-Invasive Detection of Cyclic Hypoxia in Head and Neck Squamous Cell Carcinoma Xenografts

Rafal Panek[1], Lauren C.J. Baker[2], Liam Welsh[1], Carol Box[2], Suzanne A. Eccles[2], Kate L. Newbold[1], Kevin J. Harrington[1], Maria A. Schmidt[1], Martin O. Leach[1], and Simon P. Robinson[2]

[1]*Royal Marsden NHS FT and Institute of Cancer Research, Sutton, Surrey, United Kingdom,* [2]*Institute of Cancer Research, Sutton, Surrey, United Kingdom*

Introduction: The tumour microenvironment is highly dynamic and contains subpopulations of cancer cells exposed to varying gradients of oxygen, nutrients and pH[1]. Tumour hypoxia is a recognised cause of treatment resistance, and is particularly relevant to treatment outcomes in head and neck squamous cell carcinomas (HNSCC)[2-5]. The importance of acutely hypoxic tumour cells, resulting from intermittent tumour blood flow[6], on tumour progression and radioresistance is recognised[7,8]. The potential of continuous intrinsic susceptibility (IS) MRI measurements of tumour R_2* to non-invasively detect acute, cyclic hypoxia through changes in the oxy/deoxyhaemoglobin ratio has been shown[9]. In this study we have tested the feasibility of measuring spontaneous fluctuations in tumour R_2* to identify regions with transient haemodynamic blood flow in HNSCC xenografts on a clinical 3T platform. Additionally, hyperoxia-induced ΔR_2* and tissue histology were used to spatially confirm hypoxic and perfused tumour regions.

Materials and Methods:

Imaging protocol: Adult athymic mice (n=5) were injected subcutaneously on the flank with $5x10^5$ human HNSCC CAL-27 cells stably resistant to EGFR inhibitors[10] and imaged at tumour volumes of 250 – 300 mm^3. MRI was performed at 3T (Philips Achieva, Philips Medical Systems, Best, Netherlands) using a dedicated pre-clinical asymmetric high resolution three element receive coil ("Mouse Hotel", Philips), enabling simultaneous measurements of up to three animals. Two anaesthetised mice were positioned with tumours immobilized at the centre of the coil elements. A round-end cylinder phantom (31ml, 1.5mM Gd, Dotarem, in saline) was positioned in the third coil element and used to monitor MR system stability. A gradient echo sequence with 6 echo times (temporal resolution: 30s, FA = 24°, TE = 4.6\+6.9\39.1 ms, TR = 250 ms, FOV = 200 x 200 mm^2, 3 slices, voxel size: 0.3x0.3x1.5 mm^3) was used to scan continuously for 1h. During the last 10 minutes animals breathed 100% O_2. *Immunofluorescence & Histochemistry:* Mice were administered with 60mg/kg pimonidazole i.p., followed by the perfusion marker Hoechst 33342 (15mg/kg) i.v. Vessel density (CD31), the degree of perfused vasculature (Hoechst 33342), and hypoxia (pimonidazole) were subsequently quantified on frozen tumour sections using immunohistochemistry and fluorescence microscopy. *Signal processing:* R_2* maps were calculated offline for each time point using custom-written MATLAB software (MathWorks, Natick, MA), and signal intensity decay was fitted on a pixel-by-pixel basis to a monoexponential model using a least-squares fit method. R_2* time series measured during air breathing were tested for the presence of non-random fluctuations. The following processing steps, previously described by Baudelet *et al*[9], were performed: i) linear trend subtraction, ii) calculation of windowed autocovariance functions, iii) calculation of power spectral density, iv) chi-square test of power coefficients (frequency range: 1 cycle/3 to 1/30 min^{-1}), to test if any fluctuation is different from the Gaussian noise (α=0.01). Significant non-Gaussian R_2* fluctuations were spatially mapped using binary maps, and total numbers of voxels fluctuating at three different frequency ranges (1/30-1/15;1/15-1/6;1/6-1/3 min^{-1}) determined.

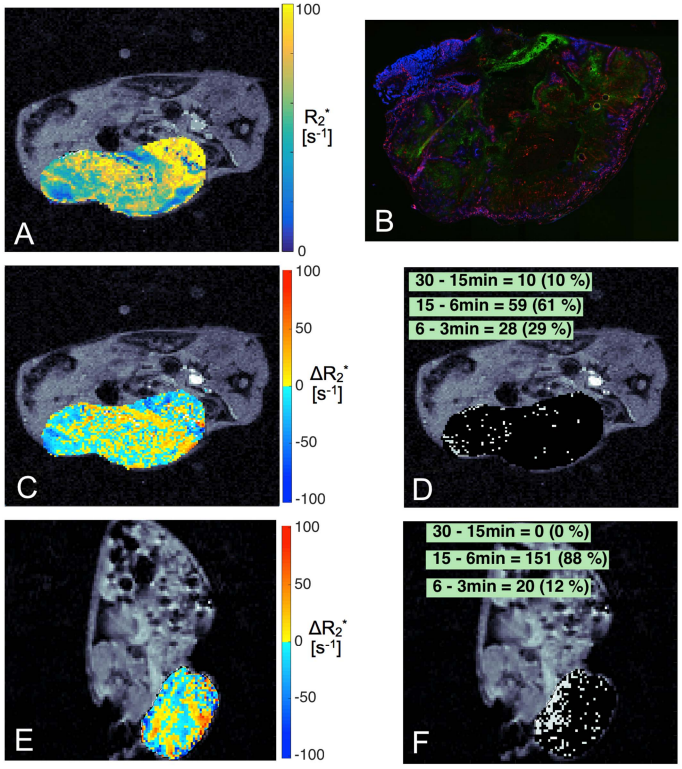

Figure 1. Representative MRI maps and histology acquired from HNSCC CAL-27 xenografts. Top and middle rows: mouse 1, bottom row: mouse 2. A: baseline map of transverse relaxation rate R_2* (air), B: composite image of a tissue section showing the distribution of Hoechst 33342 (perfusion, blue), pimonidazole (hypoxia, green) and CD31 (endothelial cell expression, red); C,E: parametric maps showing changes of the relaxation rate ΔR_2^* induced by breathing 100% O_2; D,F: binary maps showing spatial distribution of spontaneous non-Gaussian R_2* fluctuations within tumour ROI's (white voxels), with total numbers of voxels fluctuating at three different frequency ranges indicated.

Results: Initial baseline R_2* and oxygen modulated ΔR_2* maps, and binary maps of spontaneous fluctuations, acquired from central slices across two CAL-27 tumours, are shown in Figure 1. IS MRI revealed a high level of intra- and inter-tumour heterogeneity in R_2*. The median baseline tumour R_2* was 31s^{-1} (range: 22.8 - 52). Significant spontaneous R_2* variations were detected in all imaged tumours, with an average of 9% total voxels fluctuating. There were no significantly fluctuating voxels detected in the phantom region. Oxygen breathing resulted in overall slower relaxation R_2* rates, with a median difference ΔR_2* of -0.41s^{-1} (range: -3.24 - 2.34). A pronounced reduction of R_2* at the periphery of the tumour, with smaller negative or positive changes in the centre was commonly observed (Figure 1 C,E).

Discussion: Spontaneous fluctuations were detected predominantly in parts of tumours with predicted low oxygen tension, a consequence of inefficient perfusion (low negative ΔR_2*), passive oxygen diffusion (positive ΔR_2*) in the plasma or extensively leaky capillary network. The cyclical variations were also apparent in more abundant hypoxic and perfused regions of the tumour, identified using pimonidazole and Hoechst 33342 staining (Figure 1B/D), consistent with the presence of intermittent flow and fluctuating blood oxygen delivery. Hyperoxia–induced changes in R_2* were also spatially heterogeneous, and indicative of haemodynamic vasculature predominantly in the tumour periphery. The study demonstrates that acute (transient) hypoxia is detectable and quantifiable in pre-clinical tumour models *in vivo* using IS MRI. The data was acquired on a clinical 3T platform and the method has a potential to be translated into clinical work.

References: [1]Lunt *et al*, Clin Exp Met 2009;26:19-34; [2]Gatenby *et al*, IJROBP 1988;14:831-838; [3]Janssen *et al,* IJROBP 2002;54:1537-49; [4]Brizel *et al*, Radiother Oncol 1999;53:113–117; [5]Molls & Vaupel, Blood Perfusion and Microenvironment of Human Tumors. Berlin: Springer 2009:273-290; [6]Chaplin *et al*, IJROBP 1986;12:1279-1282. [7]Dewhirst *et al*, Nat Rev Cancer 2008;8:425-437; [8]Dewhirst *et al*, Radiat Res 2009;172:653-665. [9]Baudelet *et al*, Phys Med Biol 2004;49:3389-411, [10]Box C *et al*, Eur J Cancer 2013;11:2512-2521.

Acknowledgements: This work was supported by CRUK Programme Grants and MRC. The authors also acknowledge the support of CRUK and EPSRC to the Cancer Imaging Centre in association with MRC & Dept of Health and NHS funding to the NIHR Biomedicine Research Centre and the Clinical Research Facility in Imaging.